CRATERING PROCESS AFTER OBLIQUE IMPACTS. V. V. Shuvalov, Institute for Dynamics of Geospheres RAS, Leninsky pr., 38, bld.1, Moscow, 119334, Russia, shuvalov@idg.chph.ras.ru

Introduction: It is well known that most impacts are oblique, and most craters are circular [1]. Nevertheless, there are several markers, which can indicate the obliquity of impacts, and even allow estimating an impact angle [2]. The main indication of the obliquity is ejecta distribution. The distal ejecta formed at the beginning of excavation stage is the most asymmetrical feature [3] and is commonly used to determine an impact angle and direction. However, the distal ejecta is also the most short-living feature (because of a small thickness of a layer of deposits) and often can not be used to estimate the obliquity.

Another possibilities to determine a value of trajectory angle and the direction of the projectile flight for craters resulting from oblique impacts have been discussed in several recent papers. Based on geological and geophysical observations and laboratory experiments, Schultz and Anderson [4] suggested to derive impact angle and direction from second order asymmetry of impact crater itself. They applied the following features: (1) maximum central uplift offset uprange from the geometrical center, (2) breached central peak complex parallel to the trajectory, (3) large central uplift diameter relative to crater diameter, (4) larger diameter transverse to the trajectory, (5) maximum structural rim uplift transverse to the trajectory, and (6) shallower than expected excavation. However, Ekholm and Melosh [5] using Magellan data investigated two of these most frequently used criteria, (1) and (3), in studies of terrestrial craters. They found the offset distribution to be random and very similar to that for near vertical impacts, and no correlation between central peak diameter and impact angle. Even less investigated is the influence of impact angle on internal structure (target deformation and material displacement) of the crater. Numerical modelling can be a good instrument to clarify these problems, allowing us to follow the process of central peak formation and its evolution in time.

The purpose of this paper is to study the cratering process after an oblique impact using direct numerical simulations. I consider impacts of 0.5-km- and 8-km-radius asteroids, which result in formation of complex craters with central peak (0.5 km) and peak ring (8 km). An angle of trajectory inclination varies from 30 to 90 degrees (with respect to horizon). Impact velocity is assumed to be 15 km/s.

Numerical model. A 3D version of the SOVA multi-material hydrocode is used to model all stages of cratering (penetration, excavation, and modification). To model material strength the approach developed by Melosh and Ivanov [6] and O'Keefe and Ahrens [7] is used. It is based on the "rigid-plastic" model [8]. For fractured rocks (loose materials with finite cohesion), the yield strength was defined as by [9,10]

$$Y=min(Y_0+kP, Y_{max}), \quad (1)$$

where Y_0 is the cohesion, k is the coefficient of dry friction, P is the pressure, and Y_{max} is the limiting yield strength of the material at high pressure. The mechanism of acoustic fluidization [1,11] is also taken into account.

Results of simulations. Fig.1 shows a sequence of snapshots illustrating the 45 degrees impact of a 8-km-radius dunite asteroid. 50 s after the impact all projectile material has escapes from the crater, and the crater reaches its maximum depth of about 30 km. The Moho boundary (between granite crust and dunite mantle) at a depth of 32 km is deformed by the cratering flow. The central high appears approximately 100 s after the impact and it is strongly offset in the uprange direction. However, the peak of the central high move downrange and already 150 s after the impact it becomes near symmetrical, however, its internal structure remains asymmetrical. The central high reaches its maximum height (approximately 20 km) at 200 s, then it descends and spreads along the crater floor transforming into peak ring. In the final crater the Moho boundary is only slightly disturbed, but the target material from a depth of 20-25 km rises to the surface in the process of central high growth.

In all cases under consideration the central high arising is offset in the uprange direction, where crater reaches it maximum depth earlier, whereas downward motion continues in the downrange part of the crater. Later a peak of the central high moves downrange and crater surface becomes more symmetrical, but its internal structure (shown by displacement of initially horizontal layers) is not symmetrical. A displacement of the central high downrange is explained by (1) a downrange motion and displacement of central high material and (2) by an increased late rise of the crater floor in the downrange part of the crater.

The final shape (a birds eyes view) of the crater is shown in Fig.2 for the same variant as shown in Fig.1.

Discussion and conclusion. The process of cratering can roughly be divided into three stages: compression/penetration, excavation, and modification [1]. In the case of oblique impacts the penetration stage is strongly asymmetrical, occurring with dimensions comparable to projectile size. The modification stage, in contrast, is close to symmetrical because the size of the final crater (i.e., characteristic size of modification process) is considerably larger

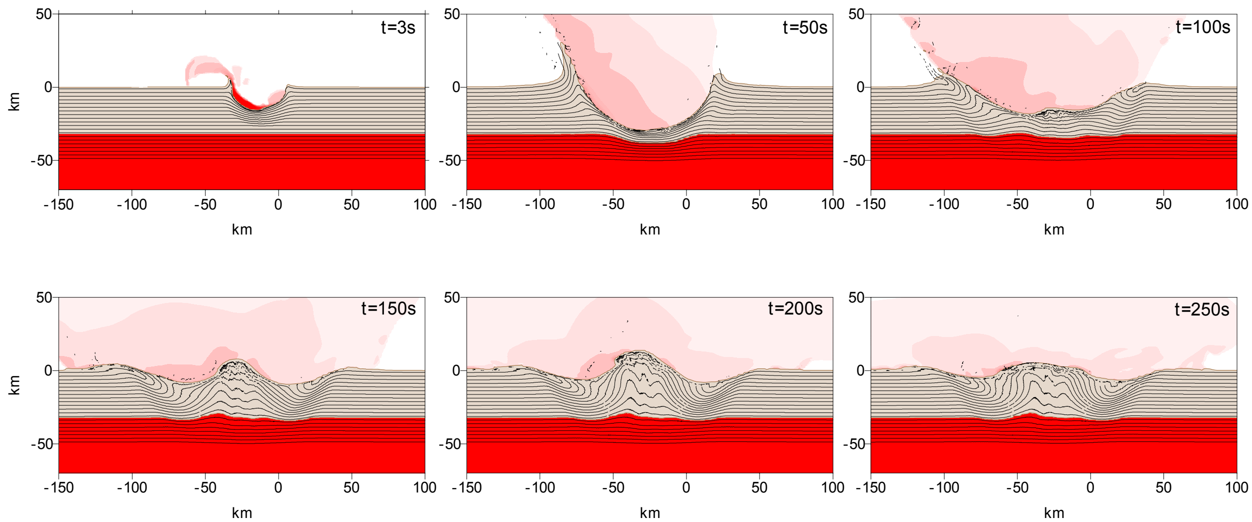

Fig.1. Impactor (red), crust (brown) and mantle (red) material distributions after a 45 degrees oblique impact of a 8-km–radius asteroid.

than the projectile size, and initial asymmetry attenuates at this distance. The excavation is an intermediate stage with early ejecta being strongly asymmetrical and late ejecta (forming crater rim) only slightly asymmetrical. Therefore we can divide all criteria of obliquity for three groups depending on governing processes. The distal ejecta, are formed at the beginning of the excavation (and the end of penetration) and its distribution is the most convincing criterion that is commonly used to determine an impact direction on other planets and satellites. The second group includes the crater rim, which is formed at the end of the excavation stage. All other criteria use second order asymmetry features formed during the modification (most symmetric) stage. Unfortunately spatial resolution is not high in these preliminary simulations and does not allow describing crater relief properly. Nevertheless the results show maximum structural rim uplift transverse to the trajectory, shallower excavation, but do not show larger diameter transverse to the trajectory. Also the numerical results substantiate the conclusion of Ekholm and Melosh [5] that an uprange offset of the central uplift probably can not be used as a criterion of obliquity. Moreover, the numerical results are believed to explain the random distribution of the offset. At the beginning of modification a transient crater is still asymmetrical and the initial uplift is offset uprange. Thereafter it moves downrange, and then uprange again. The uplift may stop at different points in these quasi-oscillations, depending on target strength, degree of acoustic fluidization, etc. In other words this effect is comparable to those resulting from both average target strength and its local fluctuations. One more important conclusion is that internal crater structure is not symmetric.

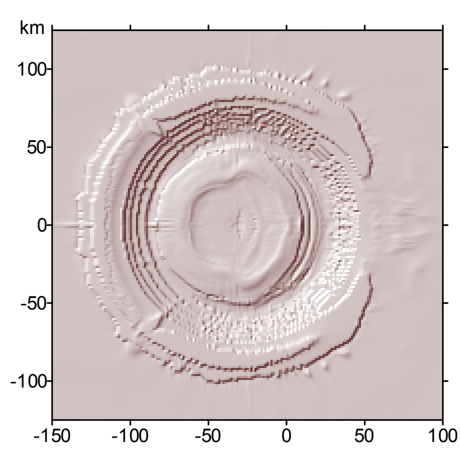

Fig.2. Final shape of the crater shown in Fig.1.

References: [1] Melosh H. J. (1989) *Impact Cratering: A Geologic Process*, 245 pp. [2] Pierazzo E. and Melosh H. J. (2000) *Annu. Rev. Earth Planet Sci., 28*, 141-167. [3] Gault D. E. and Wedekind J. A. (1978) *LPS IX*, 3843-3875. [4] Schultz P. H. and Anderson R. R. (1996) In *The Manson Impact Structure, Iowa: Anatomy of an Impact Crater, GSA Special Paper 302*, 397-417. [5] Ekholm A. G. and Melosh J. H. (2001) *Geoph. Res. Lett., 28*, 4, 623-626. [6] Melosh H. J. and Ivanov B. A. (1999) *Annu. Rev. of Earth and Planet. Sci., 27*, 385-425. [7] O'Keefe J. D. and Ahrens T. J. (1999) *JGR, 104*, 27,091–27,104. [8] Dienes J. K. and Walsh J. M. (1970) In *High-Velocity Impact Phenomena* (ed. R. Kinslow), pp.46-104. [9] Lundborg N. (1968) *Int. J. Rock. Mech. and Mining Sci., 5*, 427-454. [10] Zamyshliaev B. V. and Evterev L. S. (1990) *Models of Dynamic Deforming and Failure for Ground Media*. 215 pp., in Russian. [11] Ivanov B. A. and Turtle E. P. (2001) *LPS XXXII,* Abstract #1284.